Frontiers in Bioscience Landmark

Front. Biosci. (Landmark Ed) **2024**; 29(3): 123
https://doi.org/10.31083/j.fbl2903123

Original Research

Exploring the Role of DNA Methylation Located in Cuproptosis-Related Genes: Implications for Prognosis and Immune Landscape in Hepatocellular Carcinoma

Rui Zhu[1,2], Xue Wang[3], Fenyong Sun[1,*], Liucun Zhu[2], Wenna Guo[3,*]

[1]Department of Clinical Laboratory Medicine, Shanghai Tenth People's Hospital of Tongji University, 200072 Shanghai, China
[2]School of Life Sciences, Shanghai University, 200444 Shanghai, China
[3]School of Life Sciences, Zhengzhou University, 450001 Zhengzhou, Henan, China
*Correspondence: sunfenyong@263.net (Fenyong Sun); guowenna@zzu.edu.cn (Wenna Guo)
Academic Editor: Alessandro Poggi
Submitted: 7 October 2023 Revised: 27 January 2024 Accepted: 6 February 2024 Published: 22 March 2024

Abstract

Background: Copper dysregulation has been linked to liver disease, cardiac dysfunction, neuropathy, and anemia. Previous investigations have been undertaken to demonstrate the impact of cuproptosis-related genes (CRGs) on the poor prognosis of hepatocellular carcinoma (HCC), while the prognostic significance and beneath molecular basis of DNA-methylation sites located in CRGs remain unknown. This study aims to identify CRG-located DNA-methylation sites linked to patient prognosis and establish a novel prognostic biomarkers combination for CRG-located DNA-methylation signature. **Methods**: The prognostic biomarkers combination was established through multivariate-Cox-regression after CRG-located DNA-methylation sites tied to the outcome of patients emerged by univariate-Cox-regression. The correlation between signature and immune cell infiltration levels, immune-checkpoint-associated genes was analyzed using spearman correlation and the difference was contrasted between different groups utilizing the Mann-Whitney-U test. Real-time quantitative methylation-specific polymerase chain reaction (RT-qMSP) was used to identify gene methylation. **Results**: A novel prognostic biomarkers combination for CRG-located DNA-methylation signature was established. Subsequently, the independence of this methylation signature from clinical features and its correlation with immune infiltrative and immune checkpoints in HCC were also investigated. DNA methylation alterations can influence the onset, development, and treatment of various tumors by regulating the transcription of corresponding genes. Our analysis found that cg05706061 contained in prognosis signature was located in the promoter region of the cuproptosis-related gene *SLC31A2*. The DNA-methylation level of cg05706061 demonstrated significantly different between tumor and normal tissue, and significantly correlated with the expression of *SLC31A2*. We further investigated the promoter methylation status of *SLC31A2* by qMSP, the result showed that the DNA-methylation level of *SLC31A2* in HCC cell lines were significantly decreased compared with normal liver cells. **Conclusions**: Our findings reveal possible mechanisms of CRG-located DNA-methylation on the advancement of HCC and offers new perspectives for prognostic assessment and treatment options.

Keywords: cuproptosis; DNA methylation; prognosis; tumor microenvironment; hepatocellular carcinoma

1. Introduction

Dysregulation of copper has been associated with numerous health issues, such as liver disease, cardiac dysfunction, neuropathy, and anemia [1]. Current studies have found elevated copper levels in hepatocellular carcinoma (HCC) and increased incidence of hepatobiliary malignancies [2,3]. The pivotal role of copper contribution to the development of HCC should not be overlooked.

DNA-methylation alterations can affect various biological behaviors by regulating the transcription of corresponding genes [4], playing an imperative part in the incidence, development, and remedy of numerous carcinomas and diseases [5], including HCC [6]. Owing to its exceptional stability and usability, DNA-methylation has frequently demonstrated its suitability as diagnostic and prognostic biomarker for various tumors [7], such as HCC [8] and esophageal carcinoma (ESCA) [9]. Several research have highlighted the critical role of DNA methylation in the diagnosis, prognosis and understanding of molecular mechanisms of HCC. For instance, the significance of DNA methylation in the early detection and prognosis prediction of HCC has been comprehensively emphasized [10]. Some new differentially methylated sites were identified that could be influential in HCC [11]. A model based on 4 DNA methylation sites was developed to effectively forecast the prognosis of HCC and offer a novel pathway for personalized treatment strategies [8]. The predictive significance of a 36-DNA methylation signature was explored to pinpoint relevant epigenetic drivers and provide valuable insights into the epigenetic mechanisms underlying HCC [12]. Meanwhile, circulating tumor DNA (ctDNA) methylation markers have been discovered to be an effective tools for both diagnosing and prognosticating HCC, underscoring the potential benefits of employing non-invasive blood tests [13]. Furthermore, it has been noted that DNA methylation biomarkers exhibit better indicative and pre-

dictive performance compared to gene markers [14]. However, the impact of cuproptosis-related genes (CRGs) on the poor prognosis of HCC has been confirmed [15], while the prognostic relevance and beneath molecular basis of CRG-located DNA-methylation sites in HCC remain unknown [16].

In this study, clinical information, DNA methylation, and transcriptome data were collected from The Cancer Genome Atlas (TCGA) database. A prognostic biomarkers combination for CRG-located DNA-methylation signature was established through multivariate-Cox-regression after CRG-located DNA-methylation sites tied to the outcome of patients emerged by univariate-Cox-regression. Subsequently, the independence of methylation signature from clinical features and its correlation with immune infiltrative, immune checkpoints in HCC were investigated. This study helps uncover potential mechanisms of CRG-located DNA-methylation in HCC progression and provides new directions for prognostic assessment and treatment options for HCC.

2. Materials and Methods

2.1 Acquisition and Preprocessing of Dataset

The data with HCC were gathered by TCGA database [17], and all samples with survival information were used. The measured degrees of methylation were reported as beta values (β) [18]. CRGs were sourced from previous literature [19], and the appropriate details of DNA-methylation site were acquired from the methylation annotation file of the TCGA database. Two-thirds of the HCC patients were picked as training-cohort to find and create prognostic signature based on CRG-located DNA-methylation sites, while the remaining one-third of patients served as validation-cohort for validation of the signature.

2.2 Construction of CRG-Located DNA-Methylation Prognostic Signature

To identify sites associated with survival, Univariate-Cox-regression [20] was performed on CRG-located DNA-methylation sites. DNA-methylation sites with statistical significance were picked ($p < 0.01$) for multivariate-Cox-regression in order to form models incorporating all conceivable arrangements of 2–4 sites, aiming to screen for biomarker combinations associated with survival. Cox regression was conducted utilizing the "survival" (v.3.5-0) [21] R package. The methylation levels of CRG-located DNA-methylation sites and accompanying regression-coefficients were used calculated patient's prognostic risk score. In accordance with the median, all recipients of HCC were broken down into high- and low-risk groups.

2.3 Validation and Nomogram Construction of CRG-located DNA-Methylation Prognostic Signature

The Kaplan-Meier analysis [22] and Log-rank test were carried out to contradistinguish survival diversities between patients in low- and high-risk groups. The Receiver-operating-characteristic (ROC) curve [23] was adopted to cast the sensitivity and specificity of CRG-located DNA-methylation combinations and to judge the capacity of risk prediction models to predict HCC prognosis at 1, 3 and 5 years, which were displayed applying the "survivalROC" (v.1.0.3.1) R package. The nomogram [24] incorporating the age, clinical stage, gender, risk score and tumor grade was constructed to forecast overall survival (OS). The nomograms were created using the "rms" (v.6.5-0) R package.

2.4 Immunoassay and Functional Enrichment

The Stromal scores, ESTIMATE scores, Immune scores and immune cell infiltration levels were computed for all HCC individuals employing "CIBERSORT" [25] and "ESTIMATE" [26] R packages. The correlation between signature and immune-checkpoint-associated genes (ICGs) were analyzed using spearman correlation and the expression of ICG was contrasted between different groups utilizing the Mann-Whitney-U test. Furthermore, differentially-expressed genes (DEGs) comparing two group patients were obtained ($|\log FC| \geq 1, p < 0.01$, FC means the ratio of the gene expression value between two group). Gene ontology (GO) and Kyoto Encyclopedia of Genes and Genomes (KEGG) analysis of DEGs were carried out implementing the David [27].

2.5 DNA Isolation, Bisulfite Modification, and RT-qMSP

The LX-2 cell lines were obtained from Guangzhou Otwobio Biotech Inc (Guangzhou, China). The WRL68 and SNU449 cell lines were obtained from Shanghai Genechem Co., Ltd (Shanghai, China). The MHCC-97L and MHCC-97H cell lines were obtained from Shanghai iCell Bioscience Inc (Shanghai, China). All cell lines have been authenticated by short tandem repeat (STR) profiling. All cell lines were tested for presence of mycoplasma using the polymerase chain reaction (PCR) Mycoplasma Test Kit (Hangzhou HuaAn biotechnology Co., Ltd, Hangzhou, China, catalogue number K0103) and found to be free of contamination. These cell lines were cultured in a high sugar medium. The medium was supplemented with 10% fetal bovine serum (FBS) and 1% P/S. The cell culture was placed in an incubator, which was maintained at 37 °C and 5% CO_2 atmosphere. The cell culture was passaged every 2 days. Genomic DNA of the cell line was extracted using Animal Tissues/Cells Genomic DNA Extraction Kit (Beijing solarbio science & technology Co., Ltd., Beijing, China) and was modified by the EpiTect Fast DNA Bisulfite Kit (QIAGEN, Duesseldorf, Germany). The Light cycler 480 Real Time PCR system (Roche, Basel, Switzer-

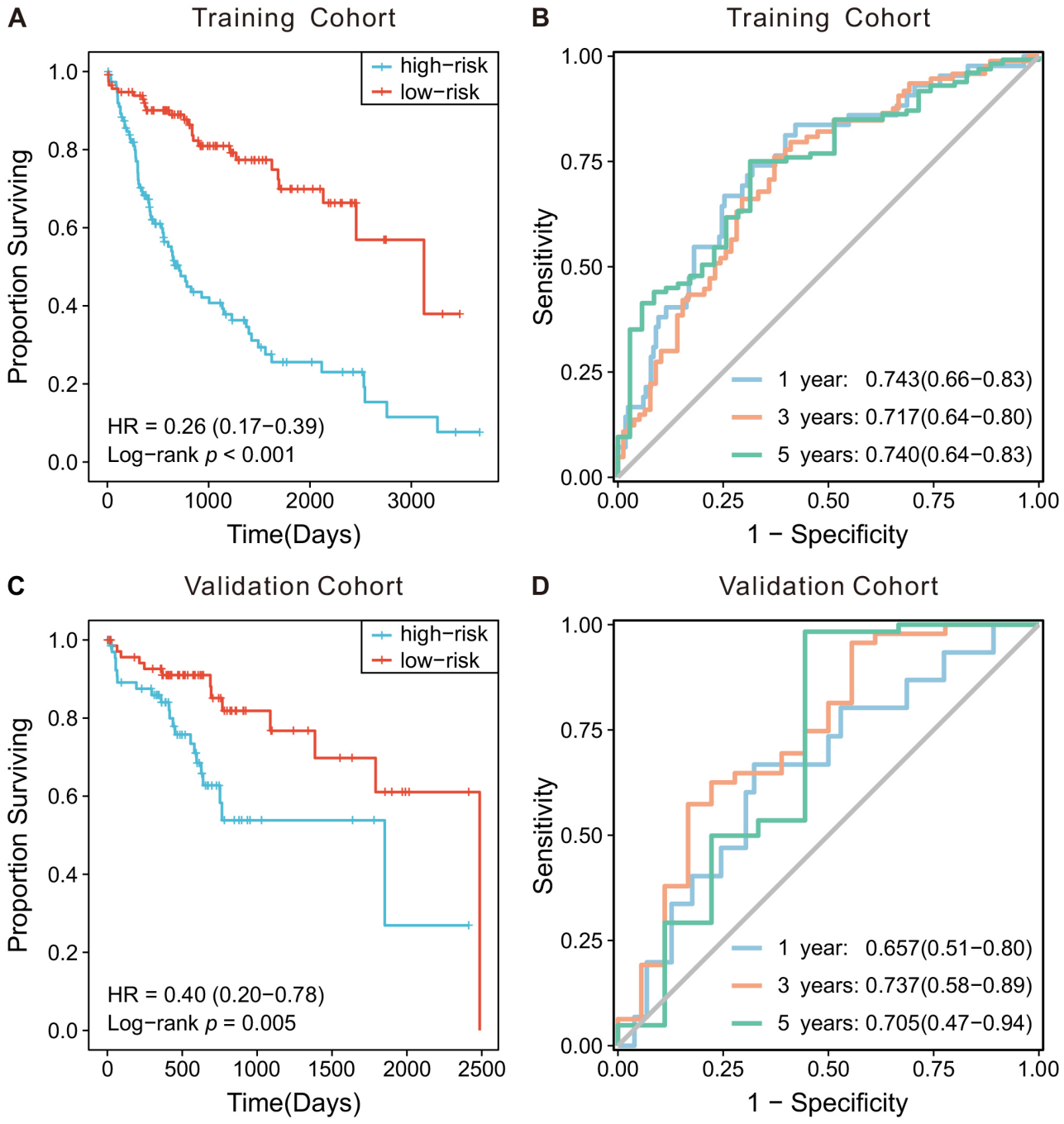

Fig. 1. Kaplan-Meier and Receiver Operating Characteristic (ROC) analyses of signature in The Cancer Genome Atlas (TCGA) training (A,B) and validation cohort (C,D). HR, the estimate of the ratio of the hazard rates between the high-risk and low-risk group.

land) was used in conjunction with the primers listed in **Supplementary Table 1** to conduct Real-time quantitative methylation-specific PCR (RT-qMSP) to identify gene methylation. The $2^{-\Delta\Delta CT}$ method, where $\Delta CT = CT_M - CT_U$ (M: methylated, U: unmethylated), was implemented to measure the methylation.

3. Results

3.1 Identifying and Establishing the CRG-Located DNA-Methylation Signature

A total of 96 CRGs were meticulously gathered through extensive literature searches, and 1374 DNA-methylation sites located in the CRGs were extracted. 277 CRG-located DNA-methylation sites that were substantially linked with prognosis were sought out employing univariate-Cox-regression, and then executed with

Table 1. The information of four CRG-located DNA methylation sites.

Probe ID	Chromosomal location	Gene symbol	*p* value[a]	coefficient[b]	*p* value[b]
cg01123518	chr16: 10743748–10743749	*NUBP1*	0.01688	17.48412	0.01459
cg05337637	chr9: 137216736–137216737	*NDOR1*	<0.001	–3.71968	<0.001
cg05398307	chr15: 74901691–74901692	*MPI*	<0.001	34.83459	<0.001
cg05706061	chr9: 113150694–113150695	*SLC31A2*	0.00782	–1.42065	0.01357

[a] Univariate Cox regression analysis.

[b] Multivariate Cox regression analysis.

multivariate-Cox-regression to create a prognostic signature. The signature comprising four CRG-located DNA-methylation sites (cg01123518, cg05337637, cg05398307, cg05706061) was selected as the best prognostic model for predicting survival through ROC analyses. The sites were linked to patient survival in both univariate- and multivariate-Cox models. These sites corresponded to the genes *NUBP1, NDOR1, MPI* and *SLC31A2*. The information of the site displays in Table 1.

3.2 Evaluating the Performance of the CRG-Located DNA-Methylation Signature

The coefficients and methylation levels were used to generate the CRG-located DNA-methylation risk score for patients. Score = (17.48412 $\times$ $\beta_{cg01123518}$) + (–3.71968 $\times$ $\beta_{cg05337637}$) + (34.83459 $\times$ $\beta_{cg05398307}$) + (–1.42065 $\times$ $\beta_{cg05706061}$). In accordance to the median, participants in the training cohort were classified into high- and low-risk groups. The Kaplan-Meier analysis revealed substantial survival disparity between them and ROC analysis demonstrated that the CRG-located DNA-methylation signature had good predictive accuracy (Fig. 1A,B). The Kaplan-Meier and ROC analysis in the validation cohort revealed a considerably decreased survival odds as risk increased (Fig. 1C,D).

3.3 Independence of the CRG-Located DNA-Methylation Signature from Clinical and Histopathological Characteristics

Age, gender, clinical stage, and tumor grade can also be used as predictors for determining HCC patient prognosis. All individuals were broken down into two groups determined by median, and it ultimately emerged that the proportion of patients in each age, clinical stage, gender, and tumor grade was relatively even in the different risk groups (Fig. 2A). To assess the independence and applicability of the signature, patients were regrouped via different clinical characteristics. The regrouping of patients according to age revealed no significant difference between the high-age and low-age group, demonstrating that the signature had no bearing on patients' age. Depending Kaplan-Meier analysis, patients in the low-risk group across all age groups had a considerably greater outcome than those in the high-risk group, and the methylation signature had superior predictive performance (Fig. 2B). Grouping patients by gender revealed that female had higher risk scores, and both male and female groups' survival rates differed drastically with different risk scores (Fig. 2C). Tumor grade is an important prognostic characteristic and categorizing patients into high-grade (G3 and G4) and low-grade (G1 and G2) cohorts found that signature effectively distinguished patients' risk for any tumor grade group (Fig. 2D). DNA methylation changes pertained with disease stage, and patient survival outcomes may vary widely even at the same stage. Due to the limited number of samples per stage, patients were split up into late-stage (III and IV) and early-stage (I and II) cohorts. Despite the fact that patients' disease severity varied greatly, there was an equally large survival variation between two risk groups at the same stage (Fig. 2E). All results demonstrate the validity of risk stratification, and the CRG methylation signature may provide a better reference for different regrouped cohorts, suggesting that this signature is an independent prognostic predictor applicable to patient survival.

3.4 Constructing A Nomogram for Survival Prediction

The independence of CRG-located DNA-methylation signatures from characteristics such as age, clinical stage, gender and tumor grade was explored using Cox regression. The findings revealed that stage and risk score were connected to OS in univariate-Cox-regression for HCC patients (Fig. 3A) and maintained strongly correlated in multivariate-Cox-regression (Fig. 3B), indicating that it might be considered as a standalone prognostic sign. The clinical characteristics and risk score were thereafter utilized to create the prediction nomogram of OS, which can provide information for clinical purposes (Fig. 3C).

3.5 Association of CRG-Located DNA-Methylation Signature with Immune

The distinct variations in immune cell infiltration between various risk groups were evaluated to understand the potential relevance of DNA-methylation signature to the immune status. The findings revealed that Stromal and ESTIMATE scores, which were considerably greater in the low-risk group, were linked adversely with risk score (Fig. 4A,B). Pursuant to the immune cell infiltration research, risk scores were strongly inversely linked with T-cells-CD4-memory-resting, T-cells-gamma-delta and Macrophages-M1, and favorably tied with T-

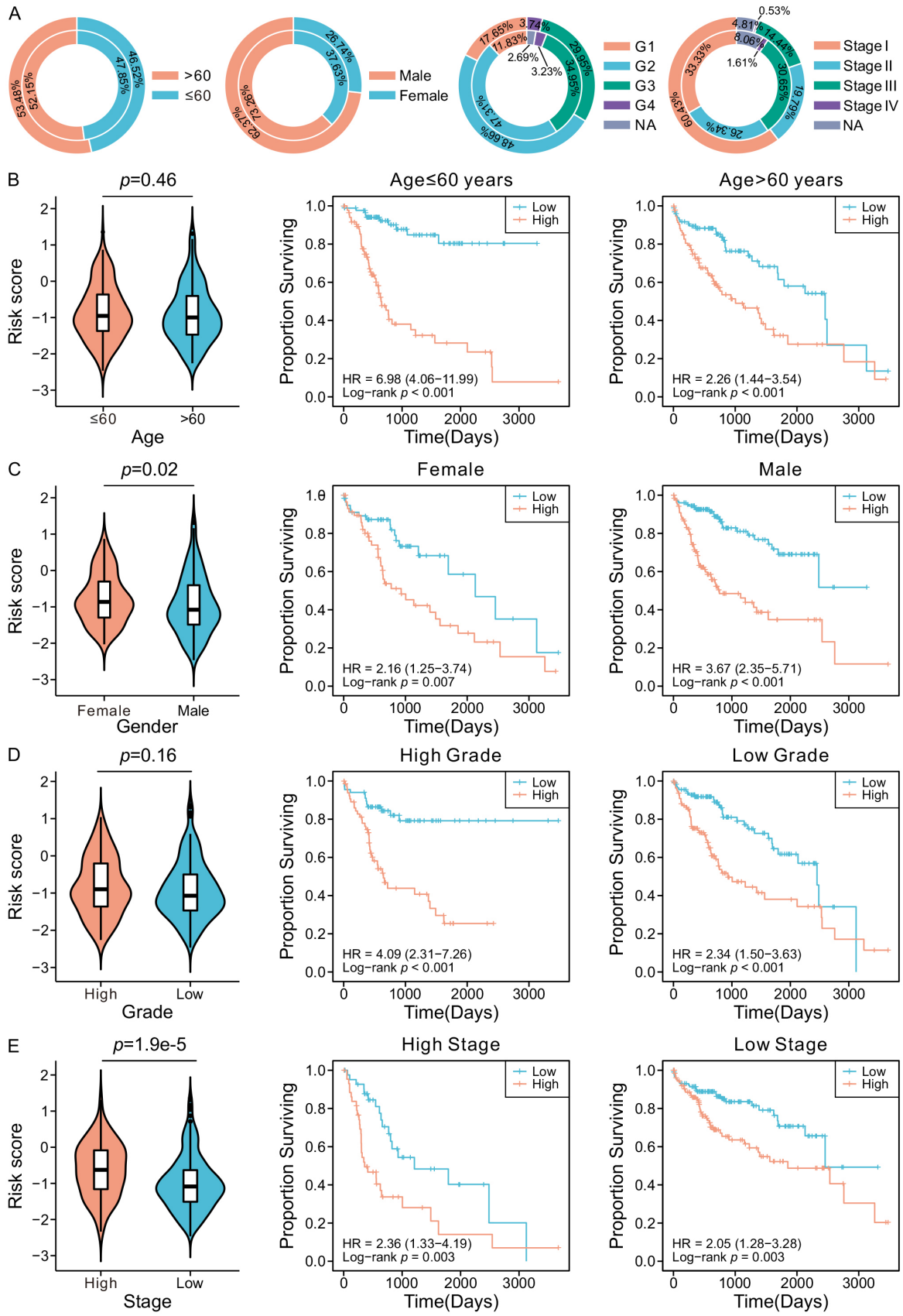

Fig. 2. The independence analysis of signature in different clinical and pathological groups. (A) Ratio of clinical characteristics. The low-risk group in outer circle, high-risk group in inner circle. (B–E) The distribution of risk score and Kaplan-Meier curves stratified by clinical characteristics.

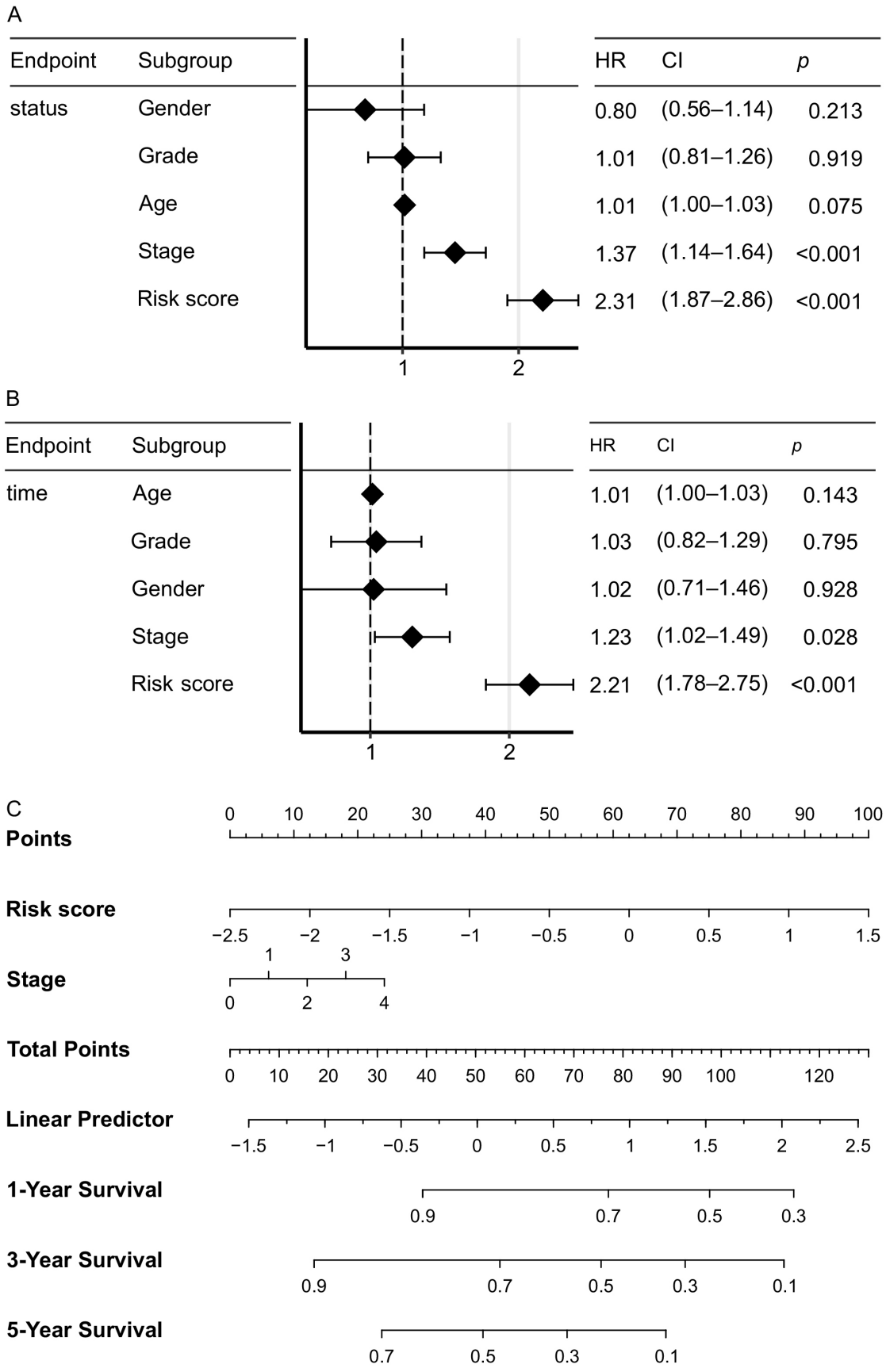

Fig. 3. The independence of signatures from clinical characteristics (A,B) and nomogram construction for the survival prediction (C).

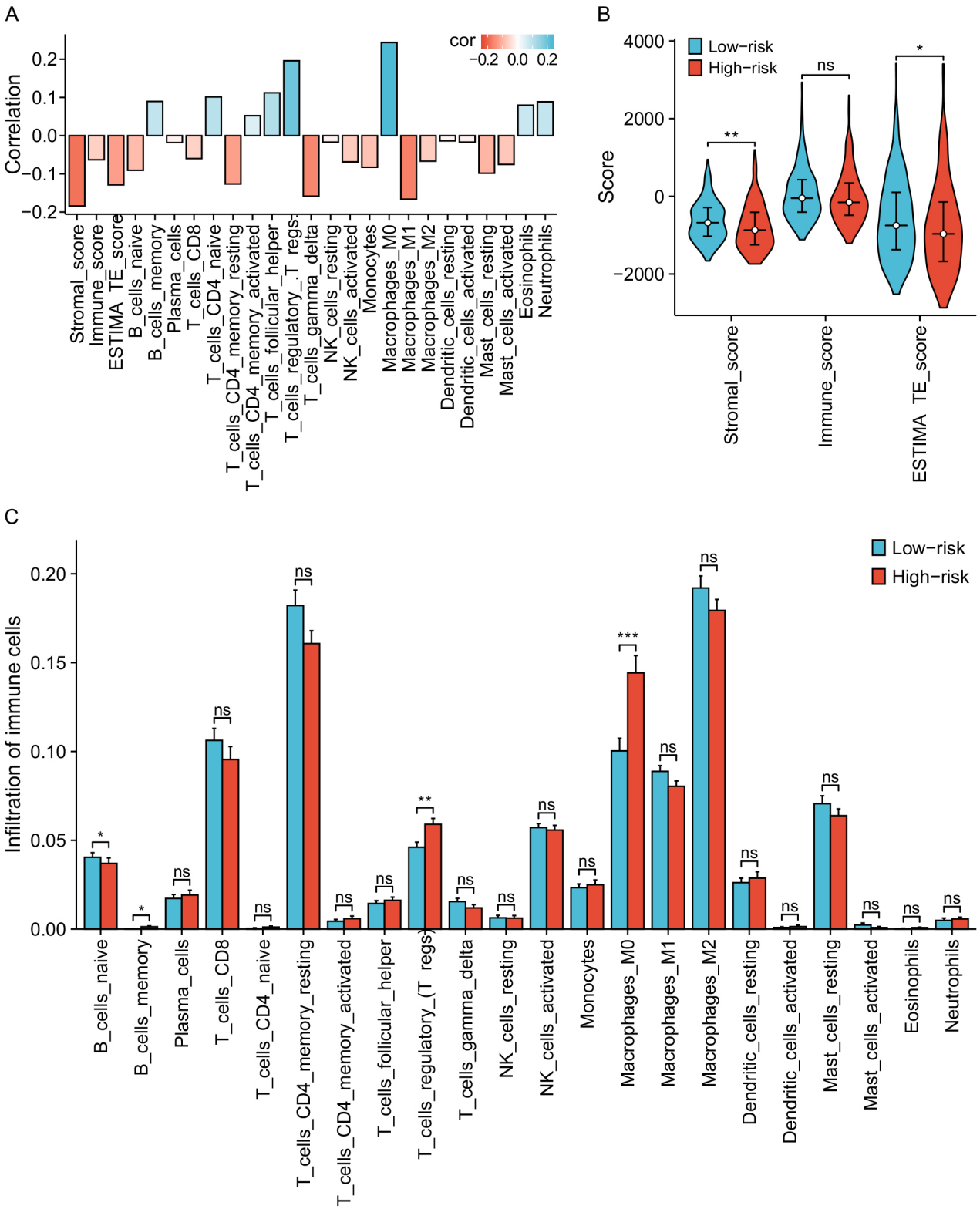

Fig. 4. The association of signature with immune (A) and expression differences between different risk hepatocellular carcinoma (HCC) patients (B,C). ns: no significance, *$p < 0.05$, **$p < 0.01$, ***$p < 0.001$.

cells-regulatory-Tregs and Macrophages-M0. The immune cell infiltration level of T-cells-regulatory-Tregs and Macrophages-M0 were drastically greater in the high-risk group (Fig. 4A,C). The checkpoint inhibitors are critical in clinical treatment and therefore the differential expression of ICGs between two risk groups was further regarded. The

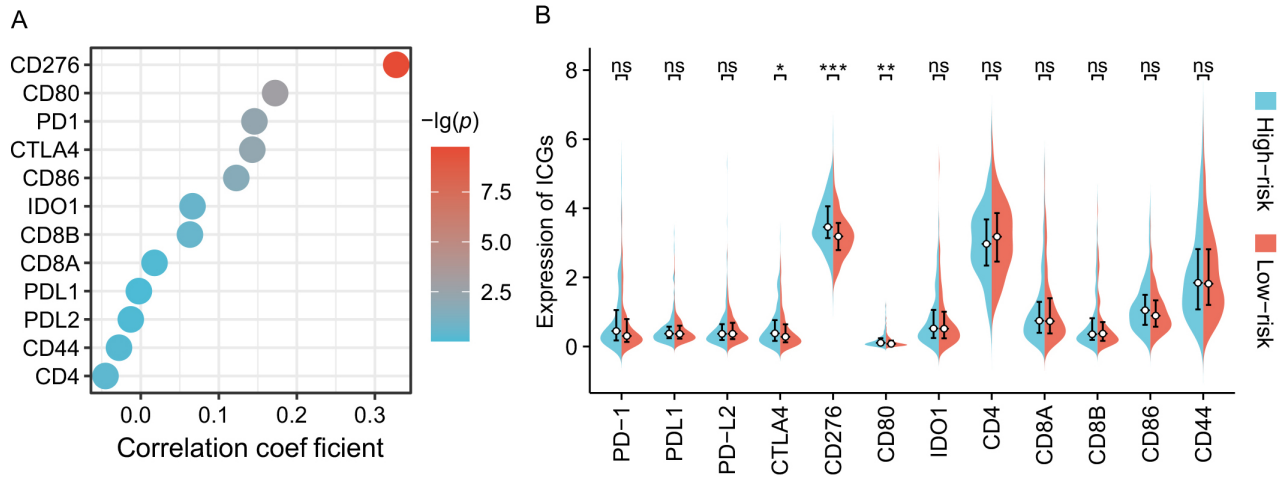

Fig. 5. The association of signature with immune-checkpoint-associated genes (ICGs) (A) and expression differences of ICGs between different risk HCC patients (B). ns: no significance, *$p < 0.05$, **$p < 0.01$, ***$p < 0.001$.

findings demonstrated an elevated relationship between risk scores and *PD-1*, *CTLA4*, *CD276*, *CD80*, *CD86* (Fig. 5A), and there were considerably distinct in *CTLA4*, *CD276*, and *CD80* between two groups (Fig. 5B). In addition, it was found that these genes participate in the cell adhesion molecules pathway, and 67% of 157 genes in the pathway are expression varied between normal and malignant tissues. These findings imply a potential link between that the CRG-located DNA-methylation signature and tumor immune microenvironment, and thus affect the prognosis of patients.

3.6 Functional Enrichment Analyses

DEGs between two risk groups were looked at in order to gain an awareness of the fundamental mechanisms in various risk groups. 1316 up-regulated genes and 35 down-regulated genes were found in the high-risk group. GO enrichment revealed that up-regulated genes were primarily linked to cation channel complex, ion channel activity, passive transmembrane transporter activity and voltage-gated potassium channel activity (Fig. 6A). KEGG pathway enrichment revealed that up-regulated genes were enriched in GABAergic synapse, glutamatergic synapse, neuroactive ligand-receptor interaction and protein digestion and absorption (Fig. 6B).

3.7 Correlation between Gene Expression and Methylation Status

DNA methylation alterations can influence the onset, development, and treatment of various tumors by regulating the transcription of corresponding genes. Our analysis found that cg05706061 contained in prognosis signature was located in the promoter region of the cuproptosis-related gene *SLC31A2* (Fig. 7A). The DNA methylation level of cg05706061 was significantly different between tumor tissue and normal tissue (**Supplementary Fig. 1**), and significantly correlated with the expression of *SLC31A2* (**Supplementary Fig. 2**). We further investigated the promoter methylation status of SLC31A2 by qMSP, the result showed that the DNA-methylation level of *SLC31A2* in HCC cell lines (SNU449, MHCC-97L and MHCC-97H) was significantly decreased compared to that in normal liver cell lines (WRL68 and LX-2 cell) ($p < 0.01$, Fig. 7B, **Supplementary Fig. 3**). Furthermore, the DNA-methylation level of *SLC31A2* exhibited a gradual decrease with increasing metastasis potential of the cell lines. The DNA-methylation levels in primary liver cancer cell line (SNU449) were significantly higher than in low metastatic cell lines (MHCC-97L) ($p < 0.01$), which were in turn significantly higher than that in high metastatic cell line (MHCC-97H) ($p < 0.05$) (Fig. 7B, **Supplementary Fig. 3**).

4. Discussion

HCC is one of the most prevalent malignancies, posing a severe threat to human health, with patients often experiencing poor clinical prognosis. Well-established risk screening and categorization tools can aid in selecting appropriate treatment options, ultimately improving overall outcomes. In this study, the cuproptosis-related gene set and TCGA dataset were combined to construct a CRG-located DNA-methylation signature with strong clinical applicability compared with the single site in HCC (**Supplementary Fig. 4**).

DNA methylation alterations can influence the onset, development, and treatment of various tumors by regulating the transcription of corresponding genes. In our study, the DNA methylation levels of cg01123518, cg05337637 and cg05706061 correlated significantly with their gene expression (**Supplementary Fig. 2**). Numerous studies argued that the attached gene of DNA-methylation site may be pivotal for cancer development. The genes corresponding

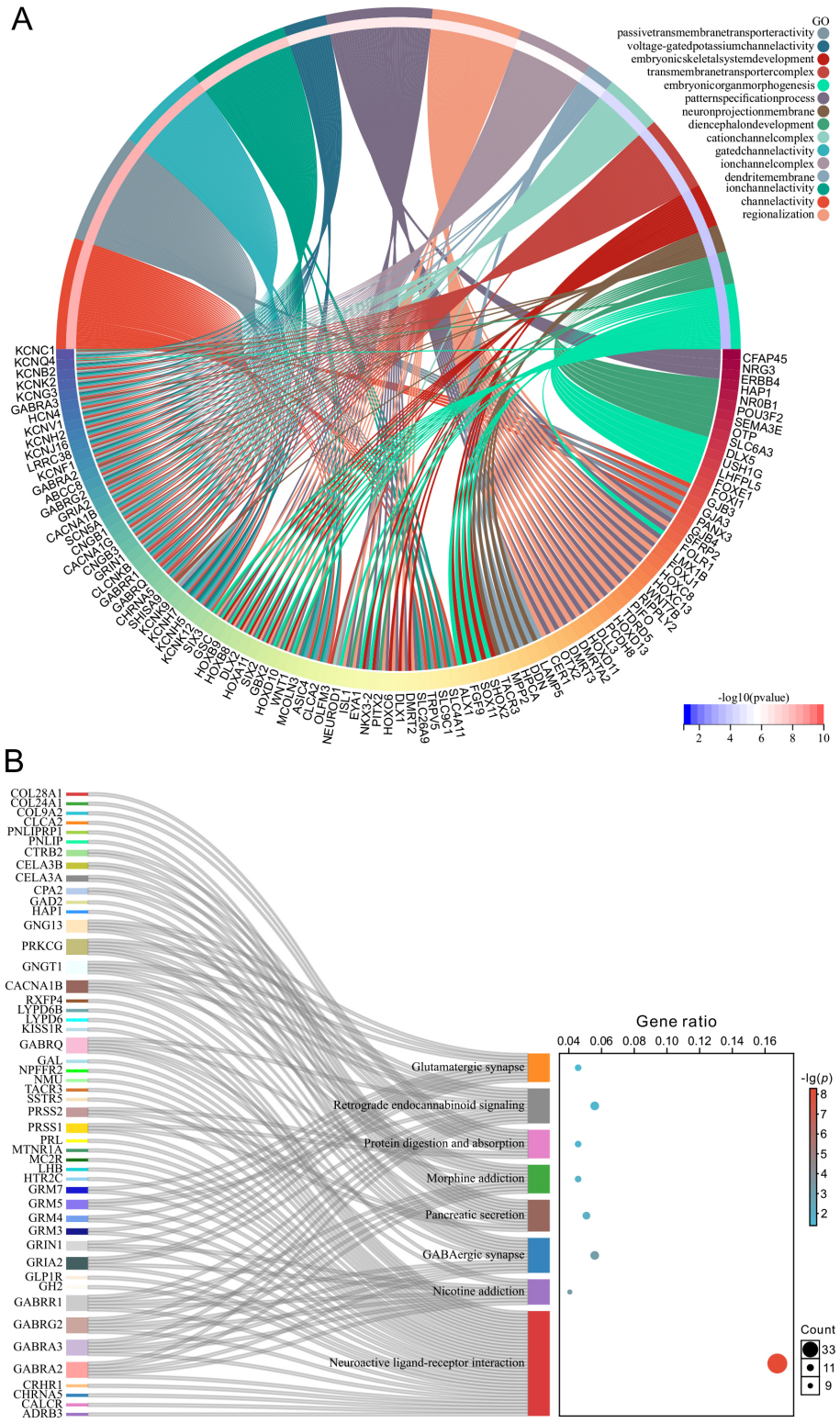

Fig. 6. The Gene ontology (GO) (A) and Kyoto Encyclopedia of Genes and Genomes (KEGG) (B) analysis of differentially-expressed genes (DEGs).

to DNA-methylation signature are *NUBP1*, *NDOR1*, *MPI* and *SLC31A2*. *NUBP1* belongs to the *NUBP*/*MRP* subfamily [28], it is involved in pathways such as netabolism and cytosolic iron-sulfur cluster assembly, as well as the cell growth regulation and cellular iron ion homeostasis [29]. The expression of *NUBP1* in colorectal cancer was markedly associated with histological type, lymph node involvement and Tumor-Node-Metastasis (TNM) staging. A

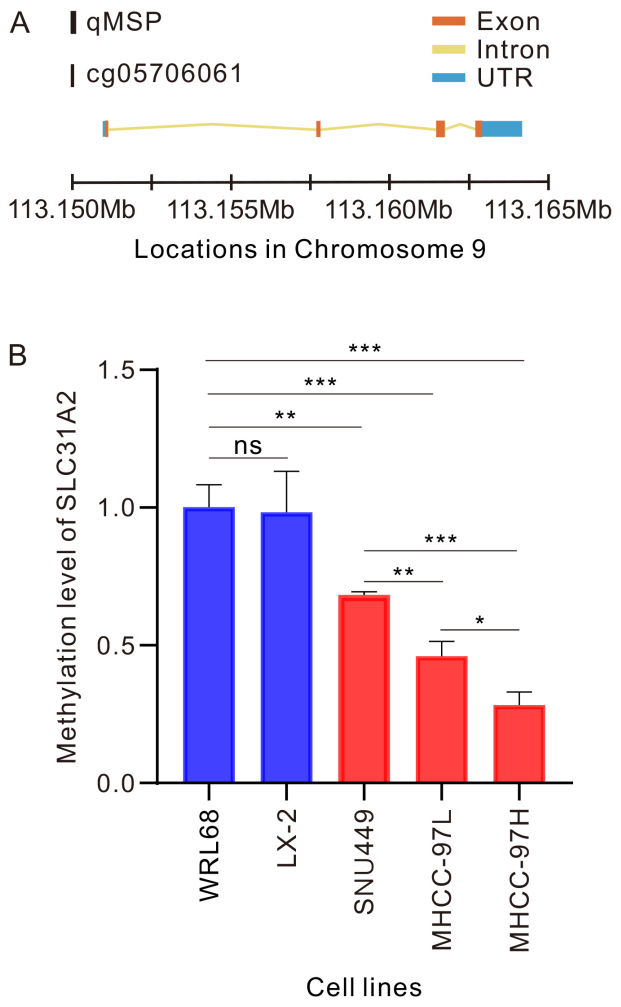

Fig. 7. The methylation level of *SLC31A2* in HCC cell lines. (A) Genomic organization of *SLC31A2* and the qMSP assay. The X-axis represents chromosome location (GRCh38). qMSP represents qMSP section location. cg05706061 represents cg05706061 site location in the promoter region of *SLC31A2*. (B) The DNA methylation level of SLC31A2 was determined by qMSP in HCC cell lines (SNU449, MHCC-97L and MHCC-97H) and control liver cell lines (WRL68 and LX2 cell). ns: no significance, *$p < 0.05$, **$p < 0.01$, ***$p < 0.001$.

negative correlation existed between *NUBP1* and OS or relapse-free survival, suggesting that *NUBP1* may serve as prognostic makers for colorectal cancer [30].

NDOR1 is a central component of the cytosolic iron-sulfur protein assembly (CIA) machinery [31], and its related pathways are cytosolic iron-sulfur cluster assembly, flavin adenine dinucleotide binding, metabolism and oxidoreductase activity. Elevated *NDOR1* expression was heavily emerged in HCC and strongly associated with HCC's poor survival [19].

MPI is a protein which can effectively link N-glycosylation and energy metabolism pathways by accelerating the interplay of Fru6P and Man6P [32], and the loss of MPI can boost radiation-induced cell death in brain malignancy [33]. Furthermore, dysfunction of MPI to operate can result in conditions such hepatic fibrosis [34], which can progress to HCC and cirrhosis [35].

SLC31A2 moves copper across cell membranes, raising the quantity of copper in the cytosol. The cellular absorption of platinum-containing cancer treatments and toxic effects of drug are both increased with decreased *SLC31A2* level [1]. Furthermore, it was discovered that *SLC31A2* was considerably changed and connected to enhanced copper levels inside liver cancer [36].

Tumor immunotherapy is a promising therapeutic approach and has made remarkable progress in recent decades, with numerous studies in basic research and clinical practice [37]. In our study, the immune scores of HCC samples were calculated to investigate the immune differences and link between immune and risk score. Additionally, several immune checkpoint genes expression were profoundly associated with risk scores. These findings reveal that heterogeneity of HCC and the tumor immune microenvironment status may be heavily shaped by the CRG-located DNA-methylation signature.

5. Conclusions

In this study, the cuproptosis-related gene set and TCGA dataset were combined to construct a CRG-located DNA-methylation signature with strong clinical applicability. Subsequently, the independence of methylation signature from clinical features and its correlation with immune infiltration, immune checkpoints in HCC were investigated. This study helps uncover potential mechanisms of CRG-located DNA-methylation in HCC progression and provides new directions for prognostic assessment and treatment options for HCC.

Abbreviations

AUC, Area Under the Curve; CRGs, Cuproptosis-Related Genes; DEGs, Differentially-Expressed Genes; HCC, Hepatocellular Carcinoma; ICGs, Immune-Checkpoint-associated Genes; *MPI*, Mannose Phosphate Isomerase; *NDOR1*, NADPH Dependent Diflavin Oxidoreductase 1; *NUBP1*, NUBP Iron-Sulfur Cluster Assembly Factor 1; OS, Overall Survival; ROC, Receiver Operating Characteristic; RT-qMSP, Real-Time quantitative Methylation-Specific Polymerase chain reaction; *SLC31A2*, Solute Carrier Family 31 Member 2; TNM, Tumor-Node-Metastasis.

Availability of Data and Materials

Data presented in this study are contained within this article and in the supplementary materials, or are available upon request to the corresponding author.

Author Contributions

WNG, LCZ and FYS designed the study. RZ conducted the data analysis and wrote the manuscript. XW designed and conducted the experiments. WNG, LCZ and FYS revised the manuscript, and final approval of the manuscript. All authors contributed to editorial changes in the manuscript. All authors read and approved the final manuscript. All authors have participated sufficiently in the work and agreed to be accountable for all aspects of the work.

Ethics Approval and Consent to Participate

Not applicable.

Acknowledgment

Not applicable.

Funding

The work was supported by grants from the National Natural Science Foundation of China (Grant No. 32070395), the National Natural Science Foundation of China (Grant No. 82302642), the National Natural Science Foundation of China (Grant No. 82103055).

Conflict of Interest

The authors declare no conflict of interest.

Supplementary Material

Supplementary material associated with this article can be found, in the online version, at https://doi.org/10.31083/j.fbl2903123.

References

[1] Öhrvik H, Nose Y, Wood LK, Kim BE, Gleber SC, Ralle M, *et al*. Ctr2 regulates biogenesis of a cleaved form of mammalian Ctr1 metal transporter lacking the copper- and cisplatin-binding ecto-domain. Proceedings of the National Academy of Sciences of the United States of America. 2013; 110: E4279–E4288.

[2] Bull PC, Thomas GR, Rommens JM, Forbes JR, Cox DW. The Wilson disease gene is a putative copper transporting P-type ATPase similar to the Menkes gene. Nature Genetics. 1993; 5: 327–337.

[3] Tanzi RE, Petrukhin K, Chernov I, Pellequer JL, Wasco W, Ross B, *et al*. The Wilson disease gene is a copper transporting ATPase with homology to the Menkes disease gene. Nature Genetics. 1993; 5: 344–350.

[4] Souren NY, Gerdes LA, Lutsik P, Gasparoni G, Beltrán E, Salhab A, *et al*. DNA methylation signatures of monozygotic twins clinically discordant for multiple sclerosis. Nature Communications. 2019; 10: 2094.

[5] Nardone S, Sams DS, Reuveni E, Getselter D, Oron O, Karpuj M, *et al*. DNA methylation analysis of the autistic brain reveals multiple dysregulated biological pathways. Translational Psychiatry. 2014; 4: e433.

[6] Long J, Chen P, Lin J, Bai Y, Yang X, Bian J, *et al*. DNA methylation-driven genes for constructing diagnostic, prognostic, and recurrence models for hepatocellular carcinoma. Theranostics. 2019; 9: 7251–7267.

[7] Roy D, Tiirikainen M. Diagnostic Power of DNA Methylation Classifiers for Early Detection of Cancer. Trends in Cancer. 2020; 6: 78–81.

[8] Hao XY, Li AQ, Shi H, Guo TK, Shen YF, Deng Y, *et al*. A novel DNA methylation-based model that effectively predicts prognosis in hepatocellular carcinoma. Bioscience Reports. 2021; 41: BSR20203945.

[9] Xi Y, Lin Y, Guo W, Wang X, Zhao H, Miao C, *et al*. Multi-omic characterization of genome-wide abnormal DNA methylation reveals diagnostic and prognostic markers for esophageal squamous-cell carcinoma. Signal Transduction and Targeted Therapy. 2022; 7: 53.

[10] Fu S, Debes JD, Boonstra A. DNA methylation markers in the detection of hepatocellular carcinoma. European Journal of Cancer (Oxford, England: 1990). 2023; 191: 112960.

[11] Zhang C, Ge S, Wang J, Jing X, Li H, Mei S, *et al*. Epigenomic profiling of DNA methylation for hepatocellular carcinoma diagnosis and prognosis prediction. Journal of Gastroenterology and Hepatology. 2019; 34: 1869–1877.

[12] Villanueva A, Portela A, Sayols S, Battiston C, Hoshida Y, Méndez-González J, *et al*. DNA methylation-based prognosis and epidrivers in hepatocellular carcinoma. Hepatology (Baltimore, Md.). 2015; 61: 1945–1956.

[13] Xu RH, Wei W, Krawczyk M, Wang W, Luo H, Flagg K, *et al*. Circulating tumour DNA methylation markers for diagnosis and prognosis of hepatocellular carcinoma. Nature Materials. 2017; 16: 1155–1161.

[14] Hoffmann F, Zarbl R, Niebel D, Sirokay J, Fröhlich A, Posch C, *et al*. Prognostic and predictive value of PD-L2 DNA methylation and mRNA expression in melanoma. Clinical Epigenetics. 2020; 12: 94.

[15] Zhou Y, Gu H, Shao B, Zhang S, Pall H, Peixoto RD, *et al*. Glycolysis-related gene dihydrolipoamide acetyltransferase promotes poor prognosis in hepatocellular carcinoma through the Wnt/β-catenin and PI3K/Akt signaling pathways. Annals of Translational Medicine. 2022; 10: 1240.

[16] Hernandez-Meza G, von Felden J, Gonzalez-Kozlova EE, Garcia-Lezana T, Peix J, Portela A, *et al*. DNA Methylation Profiling of Human Hepatocarcinogenesis. Hepatology (Baltimore, Md.). 2021; 74: 183–199.

[17] Cancer Genome Atlas Network. Comprehensive molecular portraits of human breast tumours. Nature. 2012; 490: 61–70.

[18] Su CL, Tantoh DM, Chou YH, Wang L, Ho CC, Chen PH, *et al*. Blood-Based SOX2-Promoter Methylation in Relation to Exercise and $PM_{2.5}$ Exposure among Taiwanese Adults. Cancers. 2020; 12: 504.

[19] Zhao X, Chen J, Yin S, Shi J, Zheng M, He C, *et al*. The expression of cuproptosis-related genes in hepatocellular carcinoma and their relationships with prognosis. Frontiers in Oncology. 2022; 12: 992468.

[20] Bradburn MJ, Clark TG, Love SB, Altman DG. Survival analysis part II: multivariate data analysis–an introduction to concepts and methods. British Journal of Cancer. 2003; 89: 431–436.

[21] van Dijk PC, Jager KJ, Zwinderman AH, Zoccali C, Dekker FW. The analysis of survival data in nephrology: basic concepts and methods of Cox regression. Kidney International. 2008; 74: 705–709.

[22] Dinse GE, Lagakos SW. Nonparametric estimation of lifetime and disease onset distributions from incomplete observations. Biometrics. 1982; 38: 921–932.

[23] Linden A. Measuring diagnostic and predictive accuracy in disease management: an introduction to receiver operating characteristic (ROC) analysis. Journal of Evaluation in Clinical Practice. 2006; 12: 132–139.

[24] Huo TI, Ho SY, Ko CC. Nomogram for surgical hepatocellular carcinoma: What have we missed? Liver International: Offi-

cial Journal of the International Association for the Study of the Liver. 2021; 41: 3034–3035.
[25] Newman AM, Liu CL, Green MR, Gentles AJ, Feng W, Xu Y, *et al*. Robust enumeration of cell subsets from tissue expression profiles. Nature Methods. 2015; 12: 453–457.
[26] Yoshihara K, Shahmoradgoli M, Martínez E, Vegesna R, Kim H, Torres-Garcia W, *et al*. Inferring tumour purity and stromal and immune cell admixture from expression data. Nature Communications. 2013; 4: 2612.
[27] Sherman BT, Hao M, Qiu J, Jiao X, Baseler MW, Lane HC, *et al*. DAVID: a web server for functional enrichment analysis and functional annotation of gene lists (2021 update). Nucleic Acids Research. 2022; 50: W216–W221.
[28] Nakashima H, Grahovac MJ, Mazzarella R, Fujiwara H, Kitchen JR, Threat TA, *et al*. Two novel mouse genes–Nubp2, mapped to the t-complex on chromosome 17, and Nubp1, mapped to chromosome 16–establish a new gene family of nucleotide-binding proteins in eukaryotes. Genomics. 1999; 60: 152–160.
[29] Stehling O, Netz DJA, Niggemeyer B, Rösser R, Eisenstein RS, Puccio H, *et al*. Human Nbp35 is essential for both cytosolic iron-sulfur protein assembly and iron homeostasis. Molecular and Cellular Biology. 2008; 28: 5517–5528.
[30] Liu W, Wang S, Qian K, Zhang J, Zhang Z, Liu H. Expression of family with sequence similarity 172 member A and nucleotide-binding protein 1 is associated with the poor prognosis of colorectal carcinoma. Oncology Letters. 2017; 14: 3587–3593.
[31] Camponeschi F, Ciofi-Baffoni S, Banci L. Anamorsin/Ndor1 Complex Reduces [2Fe-2S]-MitoNEET via a Transient Protein-Protein Interaction. Journal of the American Chemical Society. 2017; 139: 9479–9482.
[32] Gracy RW, Noltmann EA. Studies on phosphomannose isomerase. 3. A mechanism for catalysis and for the role of zinc in the enzymatic and the nonenzymatic isomerization. The Journal of Biological Chemistry. 1968; 243: 5410–5419.
[33] Cazet A, Charest J, Bennett DC, Sambrooks CL, Contessa JN. Mannose phosphate isomerase regulates fibroblast growth factor receptor family signaling and glioma radiosensitivity. PloS One. 2014; 9: e110345.
[34] Shtraizent N, DeRossi C, Nayar S, Sachidanandam R, Katz LS, Prince A, *et al*. MPI depletion enhances O-GlcNAcylation of p53 and suppresses the Warburg effect. eLife. 2017; 6: e22477.
[35] Ye Q, Liu Y, Zhang G, Deng H, Wang X, Tuo L, *et al*. Deficiency of gluconeogenic enzyme PCK1 promotes metabolic-associated fatty liver disease through PI3K/AKT/PDGF axis activation in male mice. Nature Communications. 2023; 14: 1402.
[36] Davis CI, Gu X, Kiefer RM, Ralle M, Gade TP, Brady DC. Altered copper homeostasis underlies sensitivity of hepatocellular carcinoma to copper chelation. Metallomics: Integrated Biometal Science. 2020; 12: 1995–2008.
[37] Liu J, Fu M, Wang M, Wan D, Wei Y, Wei X. Cancer vaccines as promising immuno-therapeutics: platforms and current progress. Journal of Hematology & Oncology. 2022; 15: 28.